ANALYTICAL APPROACH TO TRANSIENT ECT RESPONSES OF MULTILAYERED STRUCTURES

A PREPRINT

Faris Nafiah
School of Engineering
London South Bank University
103 Borough Rd,
London SE1 0AA
nafiahf@lsbu.ac.uk

September 28, 2020

ABSTRACT

Following the works of Theodoulidis in reformulating Dodd and Deeds models using series expansion, this article presents the analysis of Pulsed Eddy Current (PEC) responses above a stratified conductor. The harmonic eddy current problem is solved using reflection and transmission theory of electromagnetic waves, together with Fourier transformations to enable the analysis in both temporal and spectral domains.

1 Introduction

Analytical modelling approach lends itself well to various novel contributions in eddy current testing (ECT) and pulsed eddy current (PEC). It serves as a tool for optimisation analysis [1], inverse problem formulation [2], comparison study between ECT and PEC [3], as well as to study the underlying physical phenomena of eddy current-based NDT techniques [4, 5, 6].

The well-established Dodd and Deeds models [7] have been widely used for many eddy current-based NDT technique implementations. Many efforts can be seen in reformulating the models, such as replacing the integral expression with series expansions using truncated region eigenfunction expression (TREE) approach [8] as well as reformulating Cheng's matrix approach [9] with recursive reflection coefficient method [10]. A more recent improvement to the Dodd and Deeds model is in [11], where the approach suggested to take into account the electromagnetic interactions arising in inductively coupled systems and, thus, addresses the feedback problem.

Analytical models to yield exact responses of a PEC system by utilising Dodd and Deeds harmonic model can also be seen in the literature. In most implementations, Fourier transformations are used [12], while some efforts in using Laplace transformations can also be seen [13].

This study makes use of both TREE approach and recursive reflection coefficient to formulate the closed-form expressions of a coil above a stratified conductor. From this, the induction voltage (emf) responses of a coaxial coil for each frequencies are then obtained. The emf values are consequently transformed into time domain using Fourier analysis. Results are then compared with finite element models of the same loading parameters.

2 Harmonic eddy current field

On the basis of the reported works in [8, 10], we follow the method to analyse the magnetic vector potential of a bounded solution region, where the magnetic field is contributed by an axisymmetric coil above a multilayered conductors.

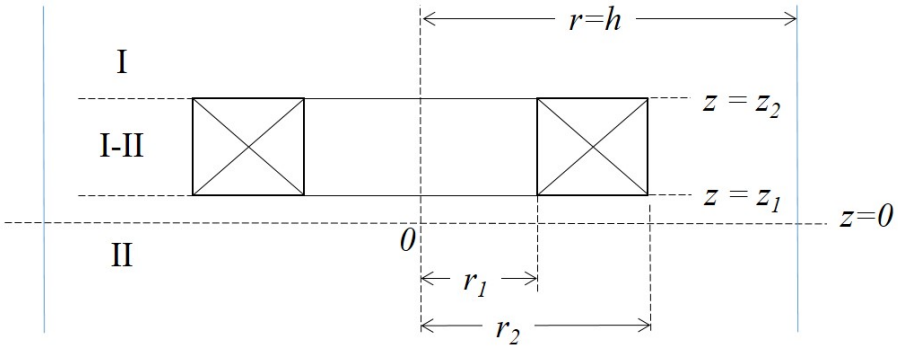

Figure 1: Isolated coil in air

2.1 Isolated coil in air

A coil of constant number of turns per unit cross-sectional area in air is considered, as a basis of the subsequent expressions, as shown in Figure 1. As depicted in the figure, the solution region is truncated at *r = h*, where an artificial boundary is placed. Region where *z* > z_2 is assigned as region I, region *z* < z_1 is region II, while the region in between z_2 and z_1 is region I-II. Imposing Dirichlet condition on the far boundary and superposition [8], the magnetic vector potential, *A* for each assigned region corresponding to the azimuthal direction θ at point *(r , z)* is

$$A_I^s(r,z) = \mu_0 \frac{T_e I(\omega)}{(r_2-r_1)(z_2-z_1)} \sum_{i=1}^{\infty} J_1(\alpha_i r) e^{-\alpha_i z} \frac{\chi(\alpha_i r_1, \alpha_i r_2)}{[(\alpha_i h) J_0(\alpha_i h)]^2 \alpha_i^2} (e^{\alpha_i z_2} - e^{\alpha_i z_1}) \tag{1}$$

$$A_{II}^s(r,z) = \mu_0 \frac{T_e I(\omega)}{(r_2-r_1)(z_2-z_1)} \sum_{i=1}^{\infty} J_1(\alpha_i r) e^{\alpha_i z} \frac{\chi(\alpha_i r_1, \alpha_i r_2)}{[(\alpha_i h) J_0(\alpha_i h)]^2 \alpha_i^2} (e^{-\alpha_i z_1} - e^{-\alpha_i z_2}) \tag{2}$$

where μ_0 is the permeability of free space, T_e is the number of turns of the excitation coil, and $I(\omega)$ is the value of current corresponding to the frequency. J_p is the p-th order Bessel function of the first kind, with the discrete eigenvalue of the problem, α_i, calculated from the equation

$$J_1(\alpha_i h) = 0 \quad \text{or} \quad J_1(x_i) = 0; \quad \alpha_i = \frac{x_i}{h}. \tag{3}$$

The term $\chi(\alpha_i r_1, \alpha_i r_2)$, on the other hand, can be calculated from

$$\chi(\alpha_i r_1, \alpha_i r_2) = \int_{\alpha_i r_1}^{\alpha_i r_2} x J_1(x) dx. \tag{4}$$

Subtituting z for z_2 in A_I^s and z for z_1 in A_{II}^s and adding them yields the magnetic vector potential, A, in region I-II

$$A_{I-II}^s(r,z) = \mu_0 \frac{T_e I(\omega)}{(r_2-r_1)(z_2-z_1)} \sum_{i=1}^{\infty} J_1(\alpha_i r) \frac{\chi(\alpha_i r_1, \alpha_i r_2)}{[(\alpha_i h) J_0(\alpha_i h)]^2 \alpha_i^2} (2 - e^{\alpha_i (z-z_2)} - e^{-\alpha_i (z-z1)}) \tag{5}$$

2.2 Coil above multilayered conductor

To consider a probe coil above a conductor, it is necessary to start off with the analysis of the incident and reflective electromagnetic waves between different mediums. The simplest example of a planar, one-dimensional inhomogeneity mediums is a half-space. From [14], the Fresnel reflection coefficient, $R_{0i,1i}$ and transmission coefficients, $T_{0i,1i}$ of a half-space, as illustrated in Figure 2, is

$$R_{0i,1i} = \frac{\mu_1 \mu_0 \alpha_i - \mu_0 \beta_i}{\mu_1 \mu_0 \alpha_i + \mu_0 \beta_i} \tag{6}$$

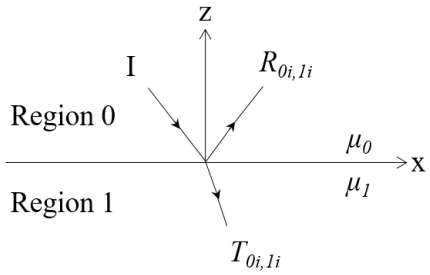

Figure 2: Reflection and transmission of a plane wave at an interface.

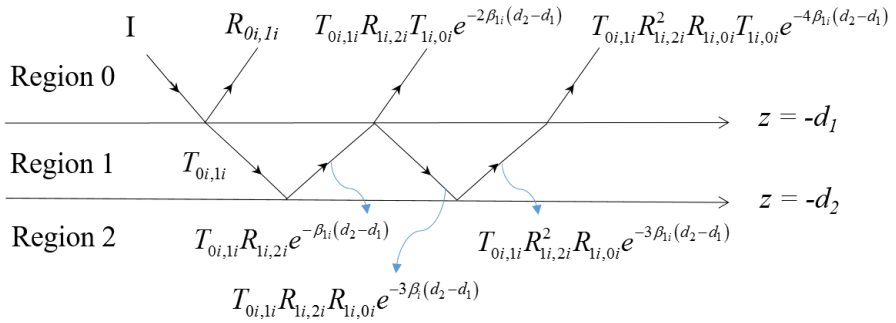

Figure 3: Geometric series of multiple reflections in a three-layer medium.

$$T_{0i,1i} = 1 + R_{0i,1i} \tag{7}$$

where μ_1 is the relative permeability of the bottom medium in the half space, and $\beta_i = \sqrt{\alpha_i^2 + j\omega\sigma_1\mu_1\mu_0}$. Note that both reflection and transmission coefficients are dependent on α_i, which varies for each iteration i in the series expansion expression. Advancing from this, the analysis of the reflection and transmitted waves of a multiple layers of mediums is extended, giving a series of reflection coefficients, as shown in Figure 3. In general, for an N-layered medium, the generalized reflection coefficient at the interface between the region n and region $n+1$ can be written as the recursive equation

$$R'_{ni,(n+1)i} = R_{ni,(n+1)i} + \frac{T_{ni,(n+1)i}R'_{(n+1)i,(n+2)i}T_{(n+1)i,i}e^{-2\beta_{(n+1)i}(d_{n+1}-d_n)}}{1 - R_{(n+1)i,(n)i}R'_{(n+1)i,(n+2)i}e^{-2\beta_{(n+1)i}(d_{n+1}-d_n)}} \tag{8}$$

where d_n is the interface location between region n and region $n+1$, $\beta_{ni} = \sqrt{\alpha_i^2 + j\omega\sigma_n\mu_n\mu_0}$, $d_{n+1} - d_n$ is the thickness of layer n, while σ_n and μ_n denote the conductivity and relative permeability of layer n respectively. Using the identity $T_{xi,yi} = 1 + R_{xi,yi}$ and $R_{xi,yi} = -R_{yi,xi}$, the expression (8) can be expressed as

$$R'_{ni,(n+1)i} = \frac{R_{ni,(n+1)i} + R'_{(n+1)i,(n+2)i}e^{-2\beta_{(n+1)i}(d_{n+1}-d_n)}}{1 + R_{ni,(n+1)i}R'_{(n+1)i,(n+2)i}e^{-2\beta_{(n+1)i}(d_{n+1}-d_n)}} \quad (n = 0,1,...,N\text{-}2). \tag{9}$$

Notice that the expression in Equation (9) is recursive relations that expresses $R'_{ni,(n+1)i}$ in terms of $R'_{(n+1)i,(n+2)i}$. For an N-layered media (N>2), $R'_{Ni,(N+1)i}$ equals zero, thus it leads to $R'_{(N-1)i,Ni} = R_{(N-1)i,Ni}$.

In eddy current-induced NDT technique, the entire magnetic field within the solution region makes up of the primary source field and the secondary-induced eddy current field. The eddy current field is regarded as the reflection and tranmission of the source field. Figure 4 visualises the geometric representation of an ECT coil above a stratified conductor. As a result, following the analysis in Section 2.1 and Equation (9), and subtituting $d_1 = 0$, the magnetic vector potential, A in azimuthal direction, θ in region I and region II (the first layer of medium) can be described as

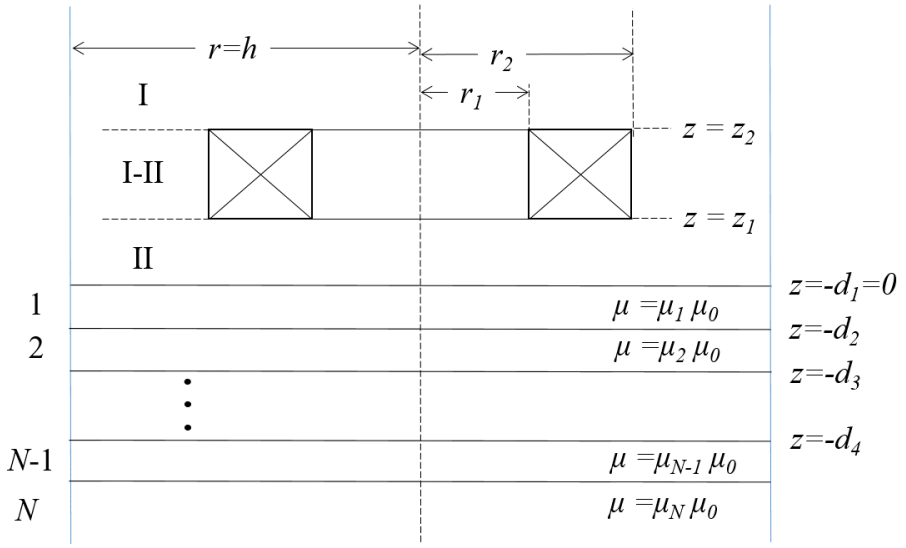

Figure 4: ECT coil above a multilayered conductor.

$$A_I(r,z) = A_I^s(r,z) + \Delta A_I^{ec}(r,z)$$
$$= A_I^s(r,z) + \mu_0 \frac{T_e I(\omega)}{(r_2-r_1)(z_2-z_1)} \sum_{i=1}^{\infty} J_1(\alpha_i r) e^{-\alpha_i z} \frac{\chi(\alpha_i r_1, \alpha_i r_2)}{[(\alpha_i h) J_0(\alpha_i h)]^2 \alpha_i^2} (e^{-\alpha_i z_1} - e^{-\alpha_i z_2}) R'_{0i,1i} \tag{10}$$

$$A_{II}(r,z) = A_{II}^s(r,z) + \Delta A_{II}^{ec}(r,z)$$
$$= A_{II}^s(r,z) + \mu_0 \frac{T_e I(\omega)}{(r_2-r_1)(z_2-z_1)} \sum_{i=1}^{\infty} J_1(\alpha_i r) e^{-\alpha_i z} \frac{\chi(\alpha_i r_1, \alpha_i r_2)}{[(\alpha_i h) J_0(\alpha_i h)]^2 \alpha_i^2} (e^{-\alpha_i z_1} - e^{-\alpha_i z_2}) R'_{0i,1i}. \tag{11}$$

$$A_{I-II}(r,z) = A_{I-II}^s(r,z) + \Delta A_{I-II}^{ec}(r,z)$$
$$= A_{I-II}^s(r,z) + \mu_0 \frac{T_e I(\omega)}{(r_2-r_1)(z_2-z_1)} \sum_{i=1}^{\infty} J_1(\alpha_i r) e^{-\alpha_i z} \frac{\chi(\alpha_i r_1, \alpha_i r_2)}{[(\alpha_i h) J_0(\alpha_i h)]^2 \alpha_i^2} (e^{-\alpha_i z_1} - e^{-\alpha_i z_2}) R'_{0i,1i}. \tag{12}$$

Notice that the field in the whole solution region consists of forward and backward travelling field. The first and second terms on the right hand sides of Equations (10) to (12) express the forward and travelling waves, respectively.

From the above analysis, the change in the magnetic vector potential above the conductors, as contributed by eddy current is

$$\Delta A^{ec}(r,z) = \mu_0 \frac{T_e I(\omega)}{(r_2-r_1)(z_2-z_1)} \sum_{i=1}^{\infty} J_1(\alpha_i r) e^{-\alpha_i z} \frac{\chi(\alpha_i r_1, \alpha_i r_2)}{[(\alpha_i h) J_0(\alpha_i h)]^2 \alpha_i^2} (e^{-\alpha_i z_1} - e^{-\alpha_i z_2}) R'_{0i,1i}. \tag{13}$$

3 Induced Voltage in a coaxial coil

3.1 Harmonic and transient induced voltage

In Section 2, it is clear that magnetic potential $A_I(r,z)$, $A_{II}(r,z)$, and $A_{I-II}(r,z)$ are dependent on the excitation current. The primary magnetic potential, $A_I^s(r,z)$, $A_{II}^s(r,z)$, and $A_{I-II}^s(r,z)$, have a linear dependency with the

excitation current for each frequency component, $I(\omega)$, while the change of magnetic vector contributed by induced current, $\Delta A^{ec}(r,z)$, is directly dependent on the excitation current frequency as seen from the term $R'_{0i,1i}$. To be methodological, the induced emf for each frequency components is first evaluated.

The voltage induced in a length of wire can be evaluated as

$$V(w) = j\omega \int A \cdot \, dS. \tag{14}$$

For an axially symmetric coil with a single loop of radius r positioned at z, Equation (14) becomes

$$V(w) = j\omega 2\pi r A(rz). \tag{15}$$

We can approximate the induced emf for a sensing coil, with T_s number of turns, r_{s2} outer radius, r_{s1} inner radius, z_{s1} lift-off and $z_{s2} - z_{s1}$ height, positioned coaxially with the excitation coil

$$\begin{aligned} V(w) &= \frac{j\omega 2\pi}{\text{coil cross section}} \iint_{\text{coil cross section}} rA(r,z)\, dr\, dz \\ &= \frac{j\omega 2\pi T_s}{(r_{s2}-r_{s1})(z_{s2}-z_{s1})} \int_{z_{s1}}^{z_{s1}} \int_{r_{s1}}^{r_{s2}} rA(r,z)\, dr\, dz, \end{aligned} \tag{16}$$

while the changes of induced emf contributed by ΔA^{ec} is

$$\Delta V^{ec}(w) = \frac{j\omega 2\pi T_s}{(r_{s2}-r_{s1})(z_{s2}-z_{s1})} \int_{z_{s1}}^{z_{s2}} \int_{r_{s1}}^{r_{s2}} r\Delta A^{ec}(r,z)\, dr\, dz, \tag{17}$$

In a bid to extend the theoretical models to using a rectangular waveform excitation current, reconstruction of time-harmonic signal using Fourier transformation is employed. The simulated rectangular current is first transformed into the frequency domain using the built-in MATLAB's "fft" command. Fast Fourier Transform break up the signal into $2M$ number of complex exponentials, corresponding to both negative and positive frequency values. The lowest frequency corresponds to $m = -M + 1$ iteration value, the highest frequency corresponds to $m = M - 1$, and the DC component corresponds to $m = 0$. The complex values of the current at each frequency components are then substituted into the term $I(w)$ in Equations (10) to (12). Consequently, the series of sinusoidal induced emf for each frequency is superimposed using Inverse Fourier Transform, where the transient induced emf, at k-th time t, can therefore be approximated as

$$V(t_k) = \frac{1}{M} \sum_{m=-M+1}^{M-1} V(w_m) e^{\frac{-2\pi}{M}[-(k-1)(m-1)]}. \tag{18}$$

3.2 Resolution of 'Gibbs phenomenon'

Spectral methods provide accurate approximations of smooth functions. However, its corresponding approximation of a piecewise smooth function is often reduced due to overshooting values near the jumps. High frequency components have large oscillations near discontinuities, which consequently yield maximum value of the partial sum. Here in our implementation, the Gibbs phenomenon is inevitable, particularly at the falling edge time of the supply current.

In order to counteract the peculiar manner of Gibbs phenomenon, we utilise the method of spectral filtering, where the Fourier series summation of Equation 18 is multiplied by the frequency order-dependent decreasing factor, $\sigma(\omega_k)$. The resulting induced emf after spectral filtering is

$$V^{(\text{filtered})}(t_k) = \frac{1}{M} \sum_{m=-M+1}^{M-1} V(w_m)\sigma(\omega_m) e^{\frac{-2\pi}{M}[-(k-1)(m-1)]}, \tag{19}$$

and the changes in emf value contributed only by the induced eddy current is

$$\Delta V^{(\text{filtered})}(t_k) = \frac{1}{M} \sum_{m=-M+1}^{M-1} \Delta V^{ec}(w_m)\sigma(\omega_m) e^{\frac{-2\pi}{M}[-(k-1)(m-1)]}, \tag{20}$$

where the term $\sigma(\omega_k)$ is obtained through various filter implementations, such as Lanczos-sigma filter

$$\sigma_1(\omega_m) = \left.\frac{sin(\pi k)}{\pi k}\right|_{m=0,1,\ldots M-1}, \tag{21}$$

exponential filter with ρ-th order

$$\sigma_2(\omega_m) = \left. e^{(ln\varepsilon_s)\omega^\rho}\right|_{m=0,1,\ldots M-1}, \tag{22}$$

and Vandeven filter with ρ-th order [15]

$$\sigma_3(\omega_m) = 1 - \frac{(2\rho-1)!}{(\rho-1)!}\left.\int_0^{|\omega|} t^{\rho-1}(1-t)^{\rho-1}dt\right|_{m=0,1,\ldots M-1}. \tag{23}$$

The convergence rate of both exponential and Vandeven filter are dependent on the order ρ. For exponential filter, ε_s represents machine zero, which in our case, is the permittivity of free space, ε_0. As seen in Equations (21) to (23), $\sigma(\omega_m)$ is evaluated only at the positive frequency components, while the induced emf is obtained in response to both negative and positive frequencies. From this, the $\sigma(\omega_m)$ at negative frequencies are simply the values at their corresponding positive frequencies.

4 Conclusions

The analytical model of transient probe response is modelled. We start off with modelling a coil on top of stratified conductor, using the reflection and transmission theory of electromagnetic waves. The obtained responses for different thicknesses hold true as justified by the underlying physical manner induced current decay.

References

[1] József Pávó and Miya Kenzo. Optimal design of eddy current testing probe using fluxset magnetic field sensors. *IEEE Transactions on Magnetics*, 32(3):1597–1600, 1996.

[2] Xingle Chen and Yinzhao Lei. Electrical conductivity measurement of ferromagnetic metallic materials using pulsed eddy current method. *NDT & E International*, 75:33–38, 2015.

[3] Xingle Chen and Yinzhao Lei. Excitation current waveform for eddy current testing on the thickness of ferromagnetic plates. *NDT & E International*, 66:28–33, sep 2014.

[4] Victor O. De Haan and Paul A. De Jong. Analytical expressions for transient induction voltage in a receiving coil due to a coaxial transmitting coil over a conducting plate. *IEEE Transactions on Magnetics*, 40(2 I):371–378, 2004.

[5] T. W. Krause, C. Mandache, and J. H V Lefebvre. Diffusion of pulsed Eddy currents in thin conducting plates. *AIP Conference Proceedings*, 975:368–375, 2008.

[6] G Y Tian, Y Li, and C Mandache. Study of Lift-Off Invariance for Pulsed Eddy-Current Signals. *IEEE Transactions on Magnetics*, 45(1):184–191, 2009.

[7] C. V. Dodd and W. E. Deeds. Analytical solutions to eddy-current probe-coil problems. *Journal of Applied Physics*, 39(6):2829–2838, 1968.

[8] Theodoros Theodoulidis and Epameinondas Kriezis. Series expansions in eddy current nondestructive evaluation models. *Journal of Materials Processing Technology*, 161(1-2 SPEC. ISS.):343–347, 2005.

[9] C. C. Cheng, C. V. Dodd, and W. E. Deeds. General analysis of probe coils near stratified conductors. *International Journal of NDT*, 3:109–130, 1971.

[10] Mengbao Fan, Pingjie Huang, Bo Ye, Dibo Hou, Guangxin Zhang, and Zekui Zhou. Analytical modeling for transient probe response in pulsed eddy current testing. *NDT & E International*, 42(5):376–383, jul 2009.

[11] D R Desjardins, T W Krause, A Tetervak, and L Clapham. Concerning the derivation of exact solutions to inductive circuit problems for eddy current testing. *NDT and E International*, 68:128–135, 2014.

[12] Yong Li, Gui Yun Tian, and Anthony Simm. Fast analytical modelling for pulsed eddy current evaluation. *NDT and E International*, 41(6):477–483, 2008.

[13] Fangwei Fu and J. R. Bowler. Transient eddy current response due to a conductive cylindrical rod. *AIP Conference Proceedings*, 894:332–339, 2007.

[14] Weng Cho Chew. Chapter 2 Planarly Layered Media. In *Wave and fields in inhomogeneous media*. Wiley-IEEE Press, 1995.

[15] Hervé Vandeven. Family of spectral filters for discontinuous problems. *Journal of Scientific Computing*, 6(2):159–192, Jun 1991.